A new leptoceratopsid dinosaur from Maastrichtian-aged deposits of the Sustut Basin, northern British Columbia, Canada

Victoria M. Arbour [Coresp., 1] , David C. Evans [2]

[1] Department of Knowledge, Royal BC Museum, Victoria, BC, Canada

[2] Department of Natural History, Royal Ontario Museum, Toronto, ON, Canada

Corresponding Author: Victoria M. Arbour
Email address: varbour@royalbcmuseum.bc.ca

A partial dinosaur skeleton from the Sustut Basin of northern British Columbia, Canada, previously described as an indeterminate neornithischian, is here reinterpreted as a leptoceratopsid ceratopsian, *Ferrisaurus sustutensis*, gen. et. sp. nov. The skeleton includes parts of the pectoral girdles, left forelimb, left hindlimb, and right pes. It can be distinguished from other named leptoceratopsids based on the proportions of the ulna and pedal phalanges. This is the first unique dinosaur species reported from British Columbia, and can be placed within a reasonably resolved phylogenetic context, with *Ferrisaurus* recovered as more closely related to *Leptoceratops* than *Montanoceratops*. At 68.2 to 67.2 Ma in age, *Ferrisaurus* falls between, and slightly overlaps with, both *Montanoceratops* and *Leptoceratops*, and represents a western range extension for Laramidian leptoceratopsids.

1 **A new leptoceratopsid dinosaur from Maastrichtian-aged deposits of the Sustut Basin, northern**

2 **British Columbia, Canada**

4 Victoria M. Arbour[1], David C. Evans[2]

6 [1]Department of Knowledge, Royal BC Museum, Victoria, BC, Canada

7 [2]Department of Natural History, Royal Ontario Museum, Toronto, ON, Canada

9 Corresponding author:

10 Victoria M. Arbour[1]

11 Email address: varbour@royalbcmuseum.bc.ca

23 **ABSTRACT**

24 A partial dinosaur skeleton from the Sustut Basin of northern British Columbia, Canada, previously

25 described as an indeterminate neornithischian, is here reinterpreted as a leptoceratopsid ceratopsian,

26 *Ferrisaurus sustutensis*, gen. et. sp. nov. The skeleton includes parts of the pectoral girdles, left forelimb,

27 left hindlimb, and right pes. It can be distinguished from other named leptoceratopsids based on the

28 proportions of the ulna and pedal phalanges. This is the first unique dinosaur species reported from

29 British Columbia, and can be placed within a reasonably resolved phylogenetic context, with *Ferrisaurus*

30 recovered as more closely related to *Leptoceratops* than *Montanoceratops*. At 68.2 to 67.2 Ma in age,

31 *Ferrisaurus* falls between, and slightly overlaps with, both *Montanoceratops* and *Leptoceratops*, and

32 represents a western range extension for Laramidian leptoceratopsids.

43

44

45

46

47   **INTRODUCTION**

48   The dense boreal forest and thrusted, folded rocks of the Canadian Cordillera present a challenging

49   environment in which to search for dinosaurs, compared to the better exposed and more easily

50   accessible outcrops in the badlands of the prairie provinces. Nevertheless, a dinosaur specimen (RBCM

51   P900) consisting of articulated and disarticulated limb and girdle elements was discovered in 1971 in the

52   remote interior mountains of north-central British Columbia (Fig. 1; Arbour and Graves 2008). These

53   bones were collected by geologist Kenny F. Larsen, who was surveying for uranium along the then in-

54   construction BC Rail line along the Sustut River, and were later donated to Dalhousie University (Halifax,

55   NS) and subsequently accessioned at the Royal British Columbia Museum in Victoria, BC. Arbour and

56   Graves (2008) described this material and identified it as an indeterminate small-bodied, bipedal

57   neornithischian, possibly representing either a pachycephalosaur or a basal ornithopod similar to

58   *Thescelosaurus*. Here we provide a new interpretation of this material and argue for its assignment to

59   Leptoceratopsidae as a new genus and species. Leptoceratopsids were short-frilled, hornless

60   ceratopsians with a maximum body length of about two-to-three meters, and form the sister group to

61   all other coronosaurian neoceratopsians (He et al. 2015). They were present in many Campanian-

62   Maastrictian aged dinosaur assemblages from Asia and North America, but are generally rare in the

63   fossil record (Ryan et al. 2012, Longrich 2016).

64   RBCM P900 is one of the only vertebrate fossils yet described from the Sustut Basin and as such is

65   significant for understanding the distribution and evolution of dinosaurs in western North America. A

66   2017 survey of the field area near the confluence of Birdflat Creek and the Sustut River recovered a

67   fragment of the Cretaceous turtle *Basilemys* at a location closely matching Larsen's original field notes,

68   suggesting that RBCM P900 most likely derived from the same outcrop (Fig 1; Arbour et al. in press). This

69   work generated new stratigraphic and palynological data that allows the provenance of this important

70   skeleton to be documented in detail for the first time. RBCM P900 is likely from the Tango Creek

71   Formation, rather that the Brothers Peak Formation as originally reported, and the new palynological

72   data suggest that the specimen is late Maastrichtian in age, allowing its morphology and biogeography

73   to be understood in a more detailed temporal context and compared to more closely related

74   leptoceratopsids.

75

76 **Institutional abbreviations:** LACM, Los Angeles County Museum; MOR – Museum of the Rockies,

77 Bozeman, Montana, USA; RBCM – Royal BC Museum, Victoria, British Columbia, Canada; Raymond M.

78 Alf Museum of Paleontology, Claremont, California, USA; ROM – Royal Ontario Museum, Toronto,

79 Ontario, Canada; TMP - Royal Tyrrell Museum of Palaeontology, Drumheller, Alberta, Canada; UALVP –

80 University of Alberta, Edmonton, Alberta, Canada; CMN, Canadian Museum of Nature, Ottawa, Ontario,

81 Canada.

82

83 **METHODS**

84 The electronic version of this article in Portable Document Format (PDF) will represent a published work

85 according to the International Commission on Zoological Nomenclature (ICZN), and hence the new

86 names contained in the electronic version are effectively published under that Code from the electronic

87 edition alone. This published work and the nomenclatural acts it contains have been registered in

88 ZooBank, the online registration system for the ICZN. The ZooBank LSIDs (Life Science Identifiers) can be

89 resolved and the associated information viewed through any standard web browser by appending the

90 LSID to the prefix http://zoobank.org/. The LSID for this publication is:

91 urn:lsid:zoobank.org:pub:D1C60A34-3632-43AD-BCE0-C93D5E26D1B0. The online version of this work is

92 archived and available from the following digital repositories: PeerJ, PubMed Central and CLOCKSS. No

93 permits were required for this study and all fossils are permanently accessioned in repositories.

94 RBCM P900 was compared to ceratopsian, pachycephalosaurid, ornithopodan, and parksosaurid

95 dinosaurs in various collections (SI 1) and the literature, and comparative measurements are provided in

96 SI 2. Photogrammetric digital models of the specimen (SI 3) were created using Agisoft Metashape 1.5.4

97 using between 50 and 200 digital photos (in RAW format, converted to TIFFs) taken with a Canon Rebel

98 XTi.

99 We assessed the phylogenetic position of RBCM P900 using the character-taxon matrix for ceratopsians

100 presented by He et al. (2015), derived from previous matrices built by Farke et al. (2014), Ryan et al.

101 (2012), and Makovicky (2001). Our matrix includes 34 taxa and 165 characters (SI 1 and 4) and was

102 compiled in Mesquite v3.04 build 725 (Maddison and Maddison 2011). We added three new characters

103 (characters 163-165) based on observations made over the course of this study. We also tested the

104 position of RBCM P900 using the character-taxon matrix presented by Morschhauser et al. (2019), with

105 no modifications to the matrix other than the addition of RBCM P900. We performed a cladistic

106   parsimony analysis on both matrices using the Traditional Search option in TNT v1.5 (Goloboff et al.

107   2008); all characters were treated as unordered and of equal weight, and we used the tree bisection

108   reconnection (TBR) swapping algorithm with 1000 replications.

109

110   **SYSTEMATIC PALAEONTOLOGY**

111   DINOSAURIA Owen, 1842

112   ORNITHISCHIA Seeley, 1888

113   NEORNITHSICHIA Cooper, 1985

114   MARGINOCEPHALIA Sereno, 1986

115   CERATOPSIA Marsh, 1890

116   NEOCERATOPSIA Sereno, 1986

117   CORONOSAURIA Sereno, 1986

118   LEPTOCERATOPSIDAE Nopcsa, 1923

119   *FERRISAURUS SUSTUTENSIS* gen. et sp. nov. urn:lsid:zoobank.org:act:A7F4267C-8CC6-49B6-8E52-

120   2C2148929B14

121   Diagnosis: *Ferrisaurus* can be differentiated from other known leptoceratopsids based on the following

122   unique combination of characters: penultimate pedal phalanges in digits III and IV are equal or subequal

123   in proximodistal length compared to the length of the preceding phalanx, rather than shorter as in all

124   other leptoceratopsids for which these elements are preserved except possibly USNM 13863

125   (*Cerasinops*); astragalus and tibia coossified, unlike all other leptoceratopsids except for AMNH 5464

126   (*Montanoceratops)*; distal end of ulna broader relative to radius length than in *Leptoceratops;* distal end

127   of ulna medially bowed, unlike the straight ulna of the penecontemporaneous Maastrichtian taxa

128   *Leptoceratops* and *Montanoceratops*, but similar to *Cerasinops* and *Prenoceratops* from the Campanian.

129   Etymology: "Iron lizard", from Latin *ferrum* (=iron) and Greek *sauros* (=lizard), in reference to the

130   specimen's discovery along a railway line, and *sustutensis* in reference to its provenance near the Sustut

131   River and within the Sustut Basin.

132   Holotype: RBCM P900, a partial skeleton consisting of a partial right coracoid, fragmentary left scapula,

133   complete left radius, distal portion of the left ulna, associated distal two thirds of the left tibia and fibula

134   and coossified astraglus and ?calcaneum, partial articulated digits III and IV of the right pes, and an

135   unprepared block removed from the posterior surface of the tibia that appears to contain four

136   metatarsals, presumably from the left pes. Previously catalogued as RBCM.EH2006.019.0001 to

137   RBCM.EH2006.019.010 and published under RBCM.EH2006.019 by Arbour and Graves (2008).

138   Locality: RBCM P900 was discovered near the confluence of Birdflat Creek and the Sustut River in the

139   Sustut Basin (Fig. 1); the bones were found loose in the rubble during construction along the BC Rail line,

140   which has since been abandoned. Fieldwork in the Sustut Basin in 2017 provided strong support for the

141   relocation of the original collection site a few hundred meters from the confluence of the Sustut River

142   and Birdflat Creek (Arbour et al. in press); exact GPS coordinates are on file at the Royal BC Museum.

143   Formation and Age: Tatlatui Member, Tango Creek Formation, Sustut Group. Palynomorphs recovered

144   from the presumed holotype locality included the Maastrichtian marker taxon *Pseudoaquilapollenites*

145   *bertillonites*, indicating an age of approximately 68.2 to 67.2 Ma for the site (Arbour et al. in press).

146   LSID: urn:lsid:zoobank.org:act:A7F4267C-8CC6-49B6-8E52-2C2148929B14

147

148   **DESCRIPTION AND COMPARISON**

149   RBCM P900 includes multiple elements in articulation, including the tibia and fibula, several pedal

150   phalanges, and potentially the metatarsals (Fig. 2). The presence of metatarsals in a block of sediment

151   removed from the posterior face of the distal tibia suggests that the skeleton may have been fully

152   articulated in situ. The bones do not appear to have suffered from brittle or plastic deformation, but

153   they have been recrystallized, obscuring the original internal bone textures.

154   We reinterpret RBCM P900 as a leptoceratopsid based on several aspects of the preserved phalanges.

155   The non-ungual phalanges are blockier and more robust in comparison to most orodromines (e.g.

156   *Orodromeus* MOR 623B), parksosaurids (e.g. *Parksosaurus* ROM 804), and pachycephalosaurids (e.g.

157   *Stegoceras* UALVP 2). The dorsal surface of the posterior articular surface in RBCM P900 is more strongly

158   pointed, and overlaps the preceding phalanx more extensively, than in other small ornithischians with

159   ginglymoid phalanges from similar stratigraphic and geographic ranges, such as parksosaurids (e.g.

160   *Parksosaurus* ROM 804) and pachycephalosaurids (e.g. *Stegoceras* UALVP 2). Ginglymoid articular

161   surfaces, and narrow, pointed unguals, also exclude identifications of this specimen as a juvenile

162   ceratopsid (e.g. *Chasmosaurus* UALVP 52613) or hadrosaurid (e.g. *Edmontosaurus annectens*, LACM

163   23504 (Prieto-Marquez, 2014), RAM 7150 (Zheng et al. 2011), Lambeosaurinae indet., TMP

164   1998.058.0001). The relatively long and robust forelimb compared to the hindlimb, as indicated by the

165   proportions of the radius and tibia, exclude RBCM P900 from being assigned to Thescelosauridae and

166   Pachycephalosauria. The preserved elements of RBCM P900 are comparable in size to large

167   leptoceratopsid specimens like *Cerasinops* MOR 300 and *Leptoceratops* CMN 8889.

168

169   **Pectoral Girdle**

170   Arbour and Graves (2008:Fig. 2:G, H) were unable to identify a thin, gently curved element of RBCM

171   P900, which we reinterpret here as a fragmentary right coracoid (Fig. 3A). Most of the edges are broken,

172   but the angle of the sternal process is complete and part of the anterior edge is complete. The

173   morphology of this bone compares well with the complete coracoids of *Leptoceratops* CMN 8889 (Fig.

174   3B); the coracoids of most other Laramidian leptoceratopsids are incomplete and cannot be compared

175   with RBCM P900. As in *Leptoceratops*, RBCM P900 had a pronounced, sharply pointed sternal process at

176   the anterior and ventral end of the coracoid. The anterior edge of the coracoid in RBCM P900 appears

177   straighter compared to the more curved edge in CMN 8889 (*Leptoceratops*), but without comparable

178   material from other taxa it is difficult to assess whether or not this is within the range of intraspecific

179   variation or a taxonomic difference.

180   A fragmentary flattened bone was interpreted as a possible rib by Arbour and Graves (2008: Fig. 2E,F)

181   and is reinterpreted here as part of the left scapula (Fig. 3C, D), representing a section near the midpoint

182   of the scapular blade. It has a teardrop-shaped cross section on one side and rapidly narrows to a thin

183   oval cross-section on the other side. The teardrop-shaped outline at one end precludes identification of

184   this element as a rib shaft, and ribs for this individual would have been much smaller and less robust,

185   whereas the proportions are more in line with the scapula of a leptoceratopsid with hindlimb

186   proportions of this size. The ventral edge of the fragment is straight, and the dorsal edge is markedly

187   concave. The scapulae of *Montanoceratops* (MOR 452) and *Prenoceratops* (TCM 2003.1.9 and TCM

188   2003.1.11; Fig. 3F) are relatively straight along their dorsal lengths, whereas the scapulae of *Cerasinops*

189   (MOR 300, Fig. 3E) and *Leptoceratops* (CMN 8889) are more concave dorsally in lateral view.

190

191 **Forelimb**

192 We agree with the identification of the radius by Arbour and Graves (2008: Fig. 2C,D). The radius is a

193 relatively simple rod-shaped bone with gently expanded proximal and distal ends and a shaft that is

194 triangular in cross section (Fig. 4A-D; Table 1). Overall, the radius of RBCM P900 is very similar to that of

195 *Leptoceratops* (Brown 1914; Fig. 4E), and it differs only in subtle aspects. The proximal end in RBCM

196 P900 is less cup-shaped compared to *Leptoceratops* (CMN 8889), and the shaft lacks the prominent

197 protuberance present near the midpoint in *Leptoceratops (*AMNH 5205; Brown 1914), although a light

198 distal tuberosity is present as in AMNH 5205. The preserved radii of *Cerasinops* (MOR 300; Fig. 4F) lack

199 distal and proximal ends, but preserve straight shafts lacking any bulges or tuberosities.

200 We reinterpret the bone previously identified by Arbour and Graves (2008: Fig. 2) as the proximal half of

201 a humerus as a partial right ulna including the distal end (Fig 5A,B; Table 1). The absence of a prominent

202 deltopectoral crest or rounded humeral head is inconsistent with its identification as a humerus. The

203 ulna is incomplete proximally, but the shaft is expanded towards the broken proximal end. Based on the

204 proportions of the radius length to ulna length in *Leptoceratops*, *Montanoceratops*, and to a lesser

205 extent *Cerasinops* (SI 2) where the radius is 75-80% of the length of the ulna, the ulna of RBCM P900

206 may have been 170-180 mm in total length. The proximal expansion of the ulna occurs approximately

207 100 mm from the base of this element in RBCM P900, compared to about 120 mm in CMN 8889

208 (Leptoceratops; about 59% of the total length from the base), 96 mm in TCM 2003.1.8(Prenoceratops;

209 67% of the length), and 125 mm in MOR 300 (Cerasinops; 62% of the length). Extrapolating a total

210 length for the ulna of RBCM P900 based on these proportions yields a total length of ~150-170 mm.

211 Comparing the width of the distal ulna to the length of the radius, the ulna of RBCM P900 was

212 proportionately wider compared to other leptoceratopsids (Fig 5, SI 2), giving it a stouter appearance.

213 The ulna shaft is a flattened oval in cross-section, and the distal end is flat and only moderately

214 expanded. A diagnostic character for *Cerasinops* proposed by Chinnery and Horner (2007) is the strong

215 medial bend of the distal part of the ulna. The distal ulna of RBCM P900 is also medially deflected (Fig.

216 5G), with the posterior edge more strongly curved than the anterior edge. The postcrania of the

217 bonebed material of *Prenoceratops* was not previously described by Chinnery (2004), but examination

218 of TCM 2003.1.8, a right ulna (Fig. 5H), indicates that *Prenoceratops* also had a medial bend to the distal

219 ulna. The ulna is straight in this region in *Leptoceratops* (CMN 8889) and *Montanoceratops* (MOR 542;

220 Fig. 5I).

221

Hindlimb

223 Approximately the distal two thirds of the right tibia and fibula are preserved, with the tibia and fibula in

224 articulation (Fig. 6A-D; Table 1). Using more complete specimens of similar size as a guide (SI 2), we

225 estimate that the tibia in RBCM P900 was likely between 310 and 330 m in length originally. The

226 astragalus and possibly the calcaneum are coossified to the tibia but the boundaries between these

227 elements are difficult to discern. The tibia and astragalus are not coossified in *Leptoceratops* (CMN 8889;

228 Fig. 6F,G), *Cerasinops* (MOR 300; Fig. 6H-J) or *Montanoceratops* (MOR 542) and in these specimens the

229 boundary between these elements is clearly discernible. Makovicky (2010) notes that the astragalus is

230 partly coossified with the tibia in *Montanoceratops (*AMNH 5465). It is unclear whether this an

231 ontogenetic phenomenon, and if it is phylogenetically significant.

232 In medial and lateral views (Fig. 6A,D) the tibia of RBCM P900 has a pronounced distal curvature that

233 was not observed in any other leptoceratopsid specimens and which does not seem to represent

234 taphonomic deformation, based on the absence of crushing or fractures on the tibia. In distal view (Fig.

235 6B), the lateral and medial malleoli are offset at a distinct angle, giving the distal face of the

236 tibia/astragalus a triangular cross section; RBCM P900 has a more pronounced edge marking the

237 confluence between the malleoli compared to the condition in *Leptoceratops* (CMN 8889), *Cerasinops*

238 (MOR 300), or *Montanoceratops* (MOR 542). The tibia of RBCM P900 is straight-sided in anterior and

239 posterior view and tapers towards the midpoint in anterior or posterior view, similar to the condition in

240 *Leptoceratops* (CMN 8889; Fig. 6F,G), and *Montanoceratops* (MOR 542), and unlike the strongly kinked

241 morphology observed in *Cerasinops* (MOR 300; Fig. 6H-J). The tibia narrows significantly along the shaft

242 and has an oval cross section at its broken proximal end. The fibula is narrow, with an oval cross section.

243 A portion of matrix removed from the anterior side of the distal tibia contains what appear to be the

244 remains of four metatarsals in cross section (Fig. 6E), but little can be said about their morphology

245 without further preparation.

246 RBCM P900 preserves a large number of pedal phalanges: III-2, III-3, and III-4, and IV-2, IV-3, IV-4, and

247 IV-5 (Fig. 7A-C; Table 2). Pedal digit III was preserved in articulation on a piece of matrix (Fig. 7A,B); digit

248 IV includes IV-2 and IV-3 preserved in articulation and IV-4 and IV-5 can be 'snapped' back into

249 articulation based on the presence of some remaining matrix on these elements (Fig. 7C). The non-

250 ungual phalanges are somewhat longer than wide, but blocky rather than elongate, and ginglymoid,

251   distinguishing them from similarly-sized small-bodied ornithischians such as Parksosaurus (Fig. 8). The

252   distinctly ginglymoid nature of the interphalangeal joints is distinct from the non-ginglymoid pedal

253   phalangeal joints in Hadrosauridae (e.g., Zheng et al. 2011).

254   In *Leptoceratops* (CMN 8889, CMN 8887), *Cerasinops* (MOR 300), and *Montanoceratops* (MOR 542) the

255   penultimate pedal phalanx of each major digit is markedly shorter in length compared to the preceding

256   phalanx (~75%-90% the length of the preceding phalanx); in RBCM P900 the penultimate and preceding

257   phalanx on digits III and IV are similar in size, with the penultimate phalanx actually being slightly longer

258   than the preceding phalanx (Table 2, SI 2). *Leptoceratops (*AMNH 5205; Brown 1914) and *Cerasinops*

259   *(*USNM 13863; Gilmore 1939, Chinnery and Horner 2007) are both illustrated with penultimate

260   phalanges subequal in length to the preceding phalanx, but these are both illustrated as line drawings

261   rather than photographs, measurements were not provided by the authors, the digits in AMNH 5205

262   were not part of an articulated pes, and neither of these specimens were measured for this study. As

263   such, it is unclear if the illustrations accurately reflect the actual morphology of the pedal digits in these

264   two specimens. The figured pes of *Udanoceratops* PIN 4046/11 (Tereschenko 2008) appears to show

265   penultimate phalanges subequal in length to the preceding phalanx in digits II-IV, but measurements

266   were not provided, and no rationale was provided for why this specimen is referred to *Udanoceratops*

267   rather than *Protoceratops*. RBCM P900 can, however, be differentiated from *Udanoceratops* by the

268   morphology of the pedal unguals, if PIN 4046/11 (Tereschenko 2008) is referable to *Udanoceratops*

269   rather than *Protoceratops*.

270   The unguals of RBCM P900 are long and narrow, with a gently curved ventral surface (Fig. 7A-C, E),

271   differing from the broad, hoof-shaped unguals of ceratopsids or the wide triangular unguals of

272   protoceratopsids (Sternberg 1951). Their overall shape is similar to the unguals of most other

273   leptoceratopsids, with the possible exception of *Udanoceratops* based on specimen PIN 4046/11 where

274   the proximal articular surface of the ungual is much wider than the distal articular surface of the

275   penultimate phalanx (Tereschenko 2008). Lateral grooves on the unguals of RBCM P900 are shallow. The

276   unguals of *Leptoceratops* specimen CMN 8889 have a longitudinal furrow on the ventral surface, but

277   these are absent in the smaller *Leptoceratops* specimen CMN 8887, and ventral furrows were not

278   observed on any other leptoceratopsid unguals examined for this study. No ventral furrows are present

279   on the unguals of RBCM P900. The unguals of RBCM P900 appear slightly deeper in lateral view

280   compared to other leptoceratopsids, but it is unclear how much this is influenced by taphonomic factors

281   (e.g. the pedal elements of *Cerasinops* MOR 300 are severely crushed), ontogeny, or body size (e.g.

282   *Montanoceratops* MOR 542 is substantially smaller than RBCM P900).

283

284   **RESULTS OF THE PHYLOGENETIC ANALYSES**

285   The phylogenetic analysis of the He et al. (2015) modified matrix recovered 7 most parsimonious

286   trees, each with a tree length of 328, a consistency index of 0.60, a retention index of 0.80, and a best

287   tree-bisection reconnection score of 326 (Fig. 8). The strict consensus tree (Fig. 8) is nearly identical to

288   that presented by He et al. (2015), with a basal grade of small-bodied ceratopsians and two derived

289   clades, Coronosauria and Leptoceratopsidae. Within Leptoceratopsidae, the recovered relationships are

290   similar to those found by He et al. (2015), with *Asiaceratops* and *Cerasinops* recovered as successive

291   sister taxa to all other leptoceratopsids, *Montanoceratops* and *Ischioceratops* as sister taxa, and

292   *Prenoceratops* as the sister taxon to an unresolved clade of the six remaining leptoceratopsids, including

293   *Ferrisaurus*. Within this clade, *Ferrisaurus* has an unresolved relationship with the North American taxa

294   *Leptoceratops*, *Gryphoceratops* and *Unescoceratops* and the Asian taxa *Udanoceratops* and

295   *Zhuchengceratops*. Poor resolution of this group is most likely because of the low number of characters

296   that could be coded for *Ferrisaurus*. In two of the seven trees, *Ferrisaurus* and *Udanoceratops* were

297   sister taxa; the position of *Ferrisaurus* differs in the other five trees. Moving *Ferrisaurus* basally in the

298   tree, outside of Coronosauria+Leptoceratopsidae, increases the tree length to 329, and moving

299   *Ferrisaurus* into Ceratopsidae increases the tree length to 331.

300   The analysis of the Morschhauser et al. (2019) unmodified matrix recovered 1110 most parsimonious

301   trees, each with a tree length of 694, a consistency index of 0.45, a retention index of 0.67, and a best

302   tree-bisection reconnection score of 688. Morschhauser et al.'s (2019) strict consensus tree shows a

303   poorly resolved sister clade to Coronosauria consisting of taxa typically recovered as leptoceratopsids in

304   other analyses plus *Koreaceratops* and *Helioceratops*. The addition of *Ferrisaurus* to this matrix collapses

305   this clade, and *Ferrisaurus* is recovered in an unresolved polytomy of leptoceratopsids plus *Aquilops*,

306   *Archaeoceratops*, *Auroraceratops*, *Helioceratops*, and *Koreaceratops*, outside of Coronosauria. In 63% of

307   the trees, *Ferrisaurus* is recovered as a leptoceratopsid in an unresolved clade consisting of *Cerasinops*,

308   *Ischioceratops*, *Leptoceratops*, *Montanoceratops*, *Prenoceratops*, *Udanoceratops*, *Zhuchengceratops*,

309   and *Gryphoceratops*+*Unescoceratops*, with *Helioceratops* as the outgroup.

310   **DISCUSSION**

311 The fact that RBCM P900, the first dinosaur specimen recovered from the Sustut Basin, is a

312 leptoceratopsid rather than one of the more commonly encountered groups in many coeval formations

313 in western North America, such as hadrosaurs, ceratopsids, or tyrannosaurs, is surprising, especially

314 given well-documented preservational biases against small-bodied dinosaurs in more fossiliferous areas

315 (Brown et al. 2013a, b; Evans et al., 2013). Most leptoceratopsid taxa are distinguished on the basis of

316 cranial morphology, especially aspects of the lower jaw anatomy (e.g., Ryan et al. 2012). However,

317 excellent postcranial material is known for many taxa, making it possible to identify diagnostic features

318 in RBCM P900 despite the absence of cranial material for this specimen. *Leptoceratops*,

319 *Montanoceratops*, and *Cerasinops* are all known from multiple partial or complete skeletons (Chinnery

320 and Weishampel 1998, Chinnery and Horner 2007, Ostrom 1978, Brown and Schlaikjer 1942, Sternberg

321 1951, Brown 1914), and *Prenoceratops* specimens described by Chinnery (2004) come from a single

322 mixed bonebed from which multiple composite skeletons have been assembled.

323 Digit proportions have been used to distinguish caenagnathids (e.g. Zanno and Sampson 2005),

324 oviraptorids (Longrich et al. 2010), and ornithomimids (Kobayashi and Barsbold 2006) at low taxonomic

325 levels, and we show that they can also be used to distinguish among leptoceratopsids. In all specimens

326 preserving partial or complete articulated pedes that we were able to personally observe and measure,

327 the penultimate phalanx (preceding the ungual) for each major digit is shorter in length than the

328 immediately preceding phalanx. In other words, pedal phalanx length decreases distally in the digit,

329 except for the unguals (Fig. 7). In *Ferrisaurus*, the penultimate phalanx is subequal in length to the

330 preceding phalanx in digits 3 and 4, and phalanx length does not decrease distally within each pedal

331 digit. This appears to be unique to *Ferrisaurus* within leptoceratopsids with two exceptions.This

332 morphology may be present in a referred specimen of *Udanoceratops* (PIN 4046/11, Tereschenko 2008,

333 although it is not clear that this specimen is not referable to *Protoceratops*, and measurements were not

334 provided. Gilmore (1913) published measurements for USNM 13863 (*Cerasinops*) and noted the length

335 of III-2 as 27.5 and III-3 as 29.5 mm; although we have not had the opportunity to observe this specimen

336 in person, a 2 millimeter length increase between III-2 and III-3 is far outside the range of variation we

337 observed in leptoceratopsids over the course of this study (Table 2, SI 2), but is within the range of

338 variation of a decrease in length between III-2 and III-3. Additionally, phalanges in digit IV show the

339 more typical reduction in length distally. We suggest it is possible that III-2 and III-3 in USNM 13863

340 were at some point transposed in their positions, despite the pes being reported as articulated at the

341 time of collection by Gilmore (1913). Longer penultimate phalanges may also be present in more basal

342 ceratopsian taxa such as *Archaeoceratops* (You and Dodson 2003), although phalangeal measurements

343   were not provided in the descriptions of this taxon; phalangeal length decreases in *Yinlong* as for

344   leptoceratopsids except *Ferrisaurus* (Han et al. 2018). Overall, the observed pattern for leptoceratopsids

345   appears to be a marked decrease in non-ungual phalangeal length in each pedal digit, with the exception

346   of *Ferrisaurus*.

347   The astragalus and tibia in RBCM P900 are coossified (Fig. 6), an unusual condition among

348   leptoceratopsids that is otherwise reportedin only one specimen of *Montanoceratops* (AMNH 5465).

349   Coossification of the astragalus and tibia could indicate advanced skeletal maturity in RBCM P900, but

350   this specimen is smaller than specimens in which the tibia and astragalus remain separate (e.g.

351   *Leptoceratops* CMN 8889, *Montanoceratops* AMNH 5205), suggesting that size alone does not explain

352   the differences in coossification patterns in leptoceratopsids. It is unclear what the ontogenetic

353   significance of this coossification represents in *Ferrisaurus*. Fusion of the ankle (distal tibia and fibula)

354   has been proposed as a diagnostic character of the small bodied thescelosaurid *Albertadromeus*

355   *syntarsus* from the Campanian of Alberta (Brown et al. 2013b), and a distinctive feature of some

356   coelophysoids such as "*Syntarsus*"/?*Coelophysis kayentakatae* (Rowe 1989), mature derived

357   ceratosaurs, such as *Cryolophosaurus* (Smith et al. 2007), and mature ankylosaurs (Coombs 1971) and

358   ceratopsids (Sues and Averianov 2009).

359   *Ferrisaurus* shares with *Cerasinops* a medially bent distal ulna (originally proposed as a diagnostic

360   character for *Cerasinops* by Chinnery and Horner 2007), a feature that is also present in *Prenoceratops*

361   (TCM 2003.1.8). This feature is not present in the Maastrichtian-aged leptoceratopsids

362   *Montanoceratops* and *Leptoceratops*, which are closest in geological age to *Ferrisaurus*. Chinnery and

363   Horner (2007) suggested that the medial deflection of the ulna in *Cerasinops*, as well as the proportions

364   and histology of the limb elements, may indicate that *Cerasinops* was primarily bipedal rather than

365   quadrupedal. Although limb proportions are more difficult to determine in *Ferrisaurus*, if the complete

366   tibia was between 310-330 mm (estimated based on more complete tibiae in *Leptoceratops* and

367   *Montanoceratops*, SI 2), then the radius of *Ferrisaurus* would have been no more than 40-43% of the

368   length of the tibia. This is less than other comparable leptoceratopsids: the radius is 50% the length of

369   the tibia in *Leptoceratops* CMN 8889, 48% in *Leptoceratops* AMNH 5205, and 47% in *Leptoceratops* CMN

370   8888, and much more than 45% in the incomplete radii of *Cerasinops* MOR 300. *Ferrisaurus* thus may

371   have had a more robust distal ulna (Fig. 5), but a shorter forelimb overall compared to *Cerasinops*,

372   suggesting that it too may have been at least facultatively bipedal. Alternately, the robusticity of the

373   ulna may be related to another aspect of its ecology, such as digging, which has been suggested in the

374   orodromine *Oryctodromeus* (Fearon and Varricchio 2015) and *Protoceratops* (Longrich 2010).

375   *Ferrisaurus* was recovered as a leptoceratopsid using the modified He et al. (2015) character matrix, and

376   as a non-coronosaurian neoceratopsian in the Morschhauser et al. (2019) matrix. Although the precise

377   relationships of *Ferrisaurus* are unresolved using the He et al. (2015) matrix, we found it to be more

378   closely related to *Leptoceratops* than *Montanoceratops* (Fig. 8). Despite their stratigraphic and

379   geographic proximity, *Leptoceratops* and *Montanoceratops* are not recovered as close relatives in recent

380   phylogenetic analyses in this analysis or by He et al. (2015) and preceding versions of that matrix.

381   *Montanoceratops* occupies a relatively basal position within Leptoceratopsidae (Makovicky 2010, Ryan

382   et al. 2012, Farke et al. 2014, He et al. 2015), and was found to be the sister taxon to *Ischioceratops* from

383   Asia by He et al. (2015). *Leptoceratops* typically occupies a more derived position and has been

384   recovered as the sister taxon to the Asian *Udanoceratops* (He et al. 2015). *Ferrisaurus* was thus

385   recovered in a more derived position within Leptoceratopsidae relative to *Montanoceratops*.

386

387   **Stratigraphic and palaeobiogeographic implications**

388   Leptoceratopsids are known from the Santonian through Maastrichtian of Laramidia (Ryan et al. 2012),

389   and the Campanian-Maastrichtian of Mongolia and China (He et al. 2015); fragmentary putative

390   leptoceratopsids have also been reported from the Cenomanian of Uzbekistan (Nessov et al. 1989), the

391   ?Coniacian-Santonian of Belgium (Godefroit et al. 2007, Longrich 2016), the Campanian of North

392   Carolina (Longrich 2016), and the Campanian of Sweden (Lindgren et al. 2007). The ancestor of the

393   leptoceratopsid lineage most likely originated in Asia (Chinnery-Allgeier and Kirkland 2010), but multiple

394   exchanges across Beringia from Asia to North America (and vice versa) may have occurred.

395   *Gryphoceratops*, the oldest taxon, derives from the Deadhorse Coulee Member of the Milk River

396   Formation, with a minimum age of about 83.7 Ma (Ryan et al. 2012). Campanian Laramidian taxa include

397   *Cerasinops* from the lower Two Medicine Formation, *Prenoceratops* from the upper Two Medicine

398   Formation of Montana and Oldman Formation of Alberta, and *Unescoceratops* from the lower Dinosaur

399   Park Formation (Chinnery 2004, Chinnery and Horner 2007, Ryan et al. 2012). Only two genera are

400   known from the Maastrichtian of Laramidia: *Montanoceratops* from the St Mary River and Horseshoe

401   Canyon formations (Brown and Schlaikjer 1942, Chinnery and Weishampel 1998, Makovicky 2001), and

402   *Leptoceratops* from the Scollard and Hell Creek formations (Sternberg 1951, Ott 2002) and the Pinyin

403   Conglomerate (McKenna and Love 1970). RBCM P900 was most likely collected from approximately 68.2

404   to 67.2 Ma sediments of the Tatlatui Member of the Tango Creek Formation, based on a recent field

405   reassessment of its original collection locality and palynomorphs recovered from that site (Arbour et al.

406   in press). This places it between the stratigraphic ranges for *Montanoceratops* (71.939 – 68 Ma) and

407   *Leptoceratops* (66.97 – 66 Ma), and slightly overlapping with the known range of *Montanoceratops*

408   (Fowler 2017).

409   Stratigraphically, *Montanoceratops* and *Leptoceratops* are the most likely taxa to which RBCM P900

410   could be referred, but multiple anatomical features distinguish RBCM P900 from both *Leptoceratops* and

411   *Montanoceratops*, including the proportions of the pedal digits, the proportions of the ulna, and the

412   medially bowed morphology of the distal ulna. RBCM P900 is also unlikely to represent an individual of

413   *Cerasinops* or *Prenoceratops;* it can be distinguished from *Cerasinops* based on the proportions of the

414   pedal digits, and from both *Cerasinops* and *Prenoceratops* based on the proportions of the ulna. These

415   morphological differences are reinforced by the stratigraphic position of *Ferrisaurus* relative to

416   *Cerasinops* and *Prenoceratops* (latest Maastrichtian, vs. middle to Upper Campanian; Chinnery and

417   Horner 2007, Chinnery 2004), given that no other dinosaur species with temporally well-resolved

418   specimens spans the middle Campanian to latest Maastrichtian elsewhere in Laramidia (e.g. Eberth et al.

419   2013, Fowler 2017). An enigmatic specimen, TMP 1982.11.1, from the Maastrichtian Willow Creek

420   Formation (Miyashita et al. 2010) has been referred to *Montanoceratops* by several authors (Ryan and

421   Currie 1998), but was considered neither a representative of *Montanoceratops*, *Leptoceratops*, or

422   *Cerasinops* by Makovicky (2010). Several additional as-yet undescribed specimens in the collections of

423   the TMP (Tanke 2007) may represent examples of either *Montanoceratops*, *Leptoceratops*, or

424   *Ferrisaurus* and their description may help clarify the differences between these three taxa or provide

425   new anatomical information for *Ferrisaurus*.

426   Leptoceratopsids are uncommon components of the dinosaurian faunas of Laramidia: even in the well-

427   sampled Dinosaur Park Formation of Alberta only a handful of leptoceratopsid specimens are known.

428   Ryan and Evans (2005) hypothesized that leptoceratopsids may have avoided the wet coastal

429   environments favoured by ceratopsids. Elsewhere in North America, *Leptoceratops* appears to be

430   present primarily in piedmont and alluvial plain palaeoenvironments and is largely absent in coastal

431   plain settings (Lehman 1987, although see Ott 2007). The Tatlatui Member of the Tango Creek

432   Formation represents an alluvial plain palaeoenvironment (Bustin and McKenzie 1989), consistent with

433   the palaeoenvironmental association documented for other Maastrichtian leptoceratopsids.

434   Interestingly, the intermontane basin occurrence of *Ferrisaurus* also supports one hypothesis outlined

435   by Lehman (1987, 2001), that leptoceratopsids, along with a few other large-bodied herbivorous taxa,

436   were inhabitants of Cordilleran highlands and adjacent piedmonts, which, in part, explains their rarity in

437   the fossil record.

438   Although today the holotype locality for *Ferrisaurus* is found at approximately 56°N today, the unusual

439   and complex translational history of the Intermontane Superterrane means its palaeolatitude may have

440   lain as much as 1600 km to the south of its current position with respect to cratonic North America, and

441   may have had approximately the same palaeolatitude (~48°N) as the southern border of Oregon and

442   Idaho (Enkin et al. 2003, van Hinsbergen et al. 2015). Despite its current apparent northern latitude, the

443   holotype of *Ferrisaurus* may actually represent one of the southernmost occurrences of

444   Leptoceratopsidae in western North America, and at minimum would have been within the currently

445   known latitudinal range of Laramidian leptoceratopsids. Regardless, RBCM P900 represents a western

446   range extension for Laramidian leptoceratopsids, and a unique occurrence within a restricted

447   intermontane basin palaeoenvironment. The identification of RBCM P900 as a unique leptoceratopsid

448   distinct from other known Laramidian taxa supports previous conclusions by Makovicky (2010) and Ryan

449   et al. (2012) that Leptoceratopsidae was a diverse but currently poorly sampled lineage of Late

450   Cretaceous ceratopsians.

451

452   **CONCLUSIONS**

453   RBCM P900, previously identified as an indeterminate bipedal neornithischian by Arbour and Graves

454   (2008), instead represents the partial skeleton of a leptoceratopsid ceratopsian similar in size to large

455   specimens of *Leptoceratops* and *Cerasinops*. Although fragmentary, this specimen can be differentiated

456   from other leptoceratopsids based on the proportions and morphology of the ulna and pedal digits, and

457   is designated the holotype of the new taxon *Ferrisaurus sustutensis*. RBCM P900 was collected from the

458   Sustut Group of the southern Sustut Basin, a large but relatively unexplored terrestrial Cretaceous basin

459   in northern British Columbia, Canada. Its recognition as a distinct species of a generally rare group of

460   small-bodied dinosaurs highlights the potential for future discoveries of unique dinosaur biodiversity

461   within the intermontane basins of the western side of the North American Cordillera.

462

463 **Supplementary Information**

464 SI 1 – Specimens examined and character statements, .docx

465 SI 2 – Comparative measurements, .csv

466 SI 3 - Photogrammetric digital models of RBCM P900 are available at Morphosource: coracoid -
467 https://doi.org/10.17602/M2/M81919, https://doi.org/10.17602/M2/M86250; scapula -
468 https://doi.org/10.17602/M2/M82514, https://doi.org/10.17602/M2/M86251; radius -
469 https://doi.org/10.17602/M2/M81854, https://doi.org/10.17602/M2/M86248; ulna -
470 https://doi.org/10.17602/M2/M81857, https://doi.org/10.17602/M2/M86249; tibia/fibula -
471 https://doi.org/10.17602/M2/M81513, https://doi.org/10.17602/M2/M86245; metatarsals -
472 https://doi.org/10.17602/M2/M86252, https://doi.org/10.17602/M2/M86253; pedal digit III -
473 https://doi.org/10.17602/M2/M81852, https://doi.org/10.17602/M2/M86246; pedal digit IV-4 -
474 https://doi.org/10.17602/M2/M86254, https://doi.org/10.17602/M2/M86255

475 SI 4 – Character-taxon matrix modified from H et al. (2015), .nex

476 SI 5 - Character-taxon matrix modified from Morschhauser et al. (2019), .nex

477

478 **ACKNOWLEDGEMENTS**

479 The RBCM P900 field locality is located on the unceded traditional territory of the Gitxsan peoples. MOR
480 300 was collected from the Wilson Hodgkiss Ranch, and MOR 542 was collected from private land
481 deeded from the Blackfeet Nation. Many thanks to D. Evans (Children's Museum of Indianapolis), Jordan
482 Mallon and Kieran Shepherd (Canadian Museum of Nature), Amy Atwater, Scott Williams, and John
483 Scannella (Museum of the Rockies), Brandon Strilisky and Caleb Brown (Royal Tyrrell Museum of
484 Palaeontology), and Carl Mehling (American Museum of Nature History) for access to specimens in their
485 collections. Peter Makovicky shared photographs of *Udanoceratops*, Kentaro Chiba, Cary Woodruff and
486 Bobby Boessenecker provided assistance with digital modelling and photogrammetry, and Derek Larson
487 provided assistance with Latinization of the genus name. Funding for this project was provided by an
488 NSERC postdoctoral fellowship, an NSERC L'Oréal-UNESCO for Women in Science fellowship
489 supplement, a National Geographic Society Waitt Grant, and a Dinosaur Research Institute grant to

490   VMA, and an NSERC Discovery Grant to DCE. Many thanks to editor Hans-Dieter Sues and reviewers

491   Andy Farke and Brenda Chinnery for constructive comments that improved the manuscript.

492

493   **LITERATURE CITED**

494   Arbour VM, Evans DC, Simon DJ, Cullen TM, Braman D. In press. Cretaceous flora and fauna of the Sustut

495   Group near the Sustut River, northern British Columbia, Canada. Canadian Journal of Earth Sciences.

496   Arbour VM, Graves MC. 2008. An ornithischian dinosaur from the Sustut Basin, north-central British

497   Columbia, Canada. Canadian Journal of Earth Sciences 45:457-463.

498   Brown B. 1914. *Leptoceratops*, a new genus of Ceratopsia from the Edmonton Cretaceous of Alberta.

499   Bulletin of the American Museum of Natural History 33:567-580.

500   Brown B, Schlaikjer EM. 1942. The skeleton of *Leptoceratops* with the description of a new species.

501   American Museum Novitates 1169:1-15.

502   Brown CM, Evans DC, Campione NE, O'Brien LJ, Eberth DA. 2013a. Evidence for taphonomic size bias in

503   the Dinosaur Park Formation (Campanian, Alberta), a model Mesozoic terrestrial alluvial-paralic system.

504   Palaeogeography, Palaeoclimatology, Palaeoecology 372:108-122.

505   Brown CM, Evans DC, Ryan MJ, Russell AP. 2013b. New data on the diversity and abundance of small-

506   bodied ornithopods (Dinosauria, Ornithischia) from the Belly River Group (Campanian) of Alberta.

507   *J*ournal of Vertebrate Paleontology **33** (3): 495

508   Bustin RM, McKenzie KJ. 1989. Stratigraphy and depositional environments of the Sustut Group,

509   southern Sustut Basin, north central British Columbia. Bulletin of Canadian Petroleum Geology **37**: 210-

510   223

511   Chinnery B. 2004. Description of *Prenoceratops pieganensis* gen. et sp. nov. (Dinosauria: Neoceratopsia)

512   from the Two Medicine Formation of Montana. Journal of Vertebrate Paleontology 24:572-590.

513   Chinnery BJ, Weishampel DB. 1998. *Montanoceratops cerorhynchus* (Dinosauria: Ceratopsia) and

514   relationships among basal neoceratopsians. Journal of Vertebrate Paleontology 18:569-585.

515   Chinnery BJ, Horner JR. 2007. A new neoceratopsian dinosaur linking North American and Asian taxa.

516   Journal of Vertebrate Paleontology 27:625-641.

517   Chinnery-Allgeier BJ, Kirkland JI. 2010. An update on the paleobiogeography of ceratopsian dinosaurs.

518   In: Ryan MJ, Chinnery-Allgeier BJ, Eberth DA (eds) New perspectives on horned dinosaurs. Indiana

519   University Press, p. 387-404.

520   Coombs W. 1971. The Ankylosauridae. PhD thesis, Columbia University, New York, 487 p.

521   Currie PJ, Holmes RB, Ryan MJ, Coy C. 2016. A juvenile chasmosaurine ceratopsid (Dinosauria,

522   Ornithischia) from the Dinosaur Park Formation, Alberta, Canada. Journal of Vertebrate Paleontology 26:

523   e1048348.

524   Eberth DA, Evans DC, Brinkman DB, Therrien F, Tanke DH, Russell LS. 2013. Dinosaur biostratigraphy of

525   the Edmonton Group (Upper Cretaceous), Alberta, Canada: evidence for climate influence. Canadian

526   Journal of Earth Sciences 50:701-726.

527   Enkin RJ, Mahoney JB, Baker J, Riesterer J, and Haskin ML. 2003. Deciphering shallow paleomagnetic

528   inclinations: 2. Implications from Late Cretaceous strata overlapping the Insular/Intermontane

529   Superterrane boundary in the southern Canadian Cordillera. Journal of Geophysical Research 108:1-19.

530   Evenchick CA, Ferri F, Mustard PS, McMechan M, Osadetz KG, Stasiuk L, Wilson NSF, Enkin RJ, Hadlari T,

531   and McNicoll VJ. 2003. Recent results and activities of the Integrated Petroleum Resource Potential and

532   Geoscience Studies of the Bowser and Sustut Basins project, British Columbia. Current Research,

533   Geological Survey of Canada 2003-A13:1-11.

534   Evans DC, Schott RK, Larson DW, Brown CM, Ryan MJ. 2013. The oldest North American

535   pachycephalosaurid and the hidden diversity of small-bodied ornithischian dinosaurs. Nature

536   Communications 4: 1-10.

537   Farke AA, Maxwell WD, Cifelli RL, Wedel MJ. 2014. A ceratopsian dinosaur from the Lower Cretaceous of

538   western North America, and the biogeography of Neoceratopsia. PLOS ONE 9:e112055.

539   Fearon JL, Varricchio DJ. 2015. Morphometric analysis of the forelimb and pectoral girdle of the

540   Cretaceous ornithopod dinosaur *Oryctodromeus cubicularis* and implications for digging. Journal of

541   Vertebrate Paleontology 35.

542 Fowler DW. 2017. Revised geochronology, correlation, and dinosaur stratigraphic ranges of the

543 Santonian-Maastrichtian (Late Cretaceous) formations of the Western Interior of North America. PLoS

544 ONE 12:e0188426.

545 Godefroit P, Lambert O. 2007. A re-appraisal of *Craspedodon lonzeensis* Dollo, 1883 from the Upper

546 Cretaceous of Belgium: the first record of a neoceratopsian dinosaur in Europe? Bulletin de l'Institut

547 Royal des sciences naturelles de Belgique, sciences de la terre 77:83-93.

548 Goloboff PA, Farris JS, Nixon KC. 2008. TNT, a free program for phylogenetic analysis. Cladistics 24:774-

549 786.

550 Gilmore CW. 1939. Ceratopsian dinosaurs from the Two Medicine Formation, Upper Cretaceous of

551 Montana. Proceedings of the United States National Museum 87:1-18.

552 Han F, Forster CA, Xu X, Clark JM. 2018. Postcranial anatomy of *Yinlong downsi* (Dinosauria: Ceratopsia)

553 from the Upper Jurassic Shishugou Formation of China and the phylogeny of basal ornithischians.

554 Journal of Systematic Palaeontology 16: 1159-1187.

555]He Y, Makovicky PJ, Wang K, Chen S, Sullivan C, Han F, Xu X. 2015. A new leptoceratopsid (Ornithischia,

556 Ceratopsia) with a unique ischium from the Upper Cretaceous of Shandong Province, China. PLOS ONE

557 10:e0144148.

558 Kobayashi Y, Barsbold R. 2006. Ornithomimids from the Nemegt Formation of Mongolia. J Paleont Soc

559 Korea 22:195-207.

560 Lehman TM. 1987. Late Maastrichtian paleoenvironments and dinosaur biogeography in the western

561 interior of North America. Palaeogeography, Palaeoclimatology, Palaeoecology 60:189-217.

562 Lehman TM. 2001. Late Cretaceous dinosaur provinciality. In Tanke DH, Carpenter K (eds) Mesozoic

563 vertebrate life: new research inspired by the paleontology of Philip J. Currie. Indiana University Press,

564 pp 310-328.

565 Lindgren J, Currie PJ, Siverson M, Rees J, Cederström P, Lindgren F. 2007. The first neoceratopsian

566 dinosaur remains from Europe. Palaeontology 50:929-937.

567 Longrich N. 2010. The function of large eyes in *Protoceratops*: a nocturnal ceratopsian? In: Ryan MJ,

568 Chinnery-Allgeier BJ, Eberth DA (eds) New Perspectives on Horned Dinosaurs: The Royal Tyrrell Museum

569 Ceratopsian Symposium. Indiana University Press, pp. 308-327.

570 Longrich NR. 2016. A ceratopsian dinosaur from the Late Cretaceous of eastern North America, and

571 implications for dinosaur biogeography. Cretaceous Research 57:199-207.

572 Longrich NR, Currie PJ, Zhi-Ming D. 2010. A new oviraptorid (Dinosauria: Theropoda) from the Upper

573 Cretaceous of Bayan Mandahu, Inner Mongolia. Palaeontology 53:945-960.

574 Maddison WP, Maddison DR. 2011. Mesquite: a modular system for evolutionary analysis. Version 3.04

575 http://mesquiteproject.org

576 Makovicky PJ. 2001. A *Montanoceratops cerorhynchus* (Dinosauria: Ceratopsia) braincase from the

577 Horseshoe Canyon Formation of Alberta. In: Tanke DH, Carpenter K, Skrepnick MW (eds) Mesozoic

578 Vertebrate Life. Indiana University Press, pp. 243-262.

579 Makovicky PJ. 2010. A redescription of the *Montanoceratops cerorhynchus* holotype, with a review of

580 referred material. In: Ryan MJ, Chinnery-Allgeier BJ, Eberth DA (eds). New perspectives on horned

581 dinosaurs. Indiana University Press, pp. 68-82.

582 Miyashita TE, Currie PJ, Chinnery-Allgeier BJ. 2010. First basal neoceratopsian from the Oldman

583 Formation (Belly River Group), southern Alberta. In: Ryan MJ, Chinnery-Allgeier BJ, Eberth DA (eds) New

584 perspectives on horned dinosaurs: the Royal Tyrrell Museum Ceratopsian Symposium. Indiana University

585 Press, Bloomington, IN, pp. 83-90.

586 Morschhauser EM, You H, Li D, Dodson P. 2019. Phylogenetic history of *Auroraceratops rugosus*

587 (Ceratopsia: Ornithischia) from the Lower Cretaceous of Gansu Province, China. Journal of Vertebrate

588 Paleontology 38, suppl 1:117-147.

589 Nessov LA, Kaznyshkina LF, Cherepanov GO. 1989. Ceratopsian dinosaurs and crocodiles of the Mesozoic

590 of Middle Asia In: Bogdanova TN, Khozatsky LI (eds) Theoretical and applied aspects of modern

591 Palaeontology. Leningrad: Nauka, pp. 144–154.

592 Ostrom JH. 1978. *Leptoceratops gracilis* from the "Lance" Formation of Wyoming. Journal of

593 Paleontology 52: 697-704.

594   Ott CJ. 2006. Cranial anatomy and biogeography of the first *Leptoceratops gracilis* (Dinosauria:

595   Ornithischia) specimens from the Hell Creek Formation, southeast Montana. In: Carpenter K (ed). Horns

596   and beaks. Indiana University Press, pp. 213-233.

597   Rowe T. 1989. A new species of the theropod dinosaur *Syntarsus* from the Early Jurassic Kayenta

598   Formation of Arizona. Journal of Vertebrate Paleontology 9:125-136

599   Ryan MJ, Evans DC. 2005. Ornithischian dinosaurs. In: Currie PJ, Koppelhus EB (eds) Dinosaur Provincial

600   Park: a spectacular ancient ecosystem revealed. Indiana University Press, pp. 312-348.

601   Ryan MJ, Currie PJ. 1998. First report of protoceratopsians (Neoceratopsia) from the Late Cretaceous

602   Judith River Group, Alberta, Canada. Canadian Journal of Earth Sciences 35:820-826.

603   Ryan MJ, Evans DC, Currie PJ, Brown CM, Brinkman D. 2012. New leptoceratopsids from the Upper

604   Cretaceous of Alberta, Canada. Cretaceous Research 35:69-80.

605   Smith ND, Makovicky PJ, Hammer WR, Currie PJ. 2007. Osteology of *Cryolophosaurus ellioti* (Dinosauria:

606   Theropoda) from the Early Jurassic of Antarctica and implications for early theropod evolution.

607   Zoological Journal of the Linnean Society 151:377-421..

608   Sternberg CM. 1951. Complete skeleton of *Leptoceratops gracilis* Brown from the Upper Edmonton

609   Member on Red Deer River, Alberta. National Museum of Canada Bulletin, Annual Report 123:225-255.

610   Sues H-D, Averianov A. 2009. *Turanoceratops tardabilis* - the first ceratopsid dinosaur from Asia.

611   Naturwissenschaften 96:645-652.

612   Tanke DH. 2007. Ceratopsian discoveries and work in Alberta, Canada: Historical review and census. In

613   Braman DR, comp., Ceratopsian Symposium: Short Papers, Abstracts, and Programs. CD ROM appendix.

614   Drumheller: Royal Tyrrell Museum of Palaeontology.

615   Tereschenko VS. 2008. Adaptive features of protoceratopoids (Ornithischia: Neoceratopsia).

616   Paleontological Journal 42:273-286.

617   van Hinsbergen DJJ, de Groot LV, van Schaik SJ, Spakman W, Bijl PK, Sluijs A, Langereis CG, Brinkuis H.

618   2015. A paleolatitude calculator for paleoclimate studies. PLOS ONE 10:e0126946.

619   Xu X, Forster CA, Clark JM, Mo J. 2006. A basal ceratopsian with transitional features from the Late

620   Jurassic of northwestern China. Proceedings of the Royal Society B 273:2135-2140.

621   You H-L, Tanoue K, Dodson P. A new species of *Archaeoceratops* (Dinosauria: Neoceratopsia) from the

622   Early Cretaceous of the Mazongshan area, northwestern China. New Perspectives on Horned Dinosaurs.

623   You H.–L., Dodson P. 2003. Redescription of neoceratopsian dinosaur *Archaeoceratops* and early

624   evolution of Neoceratopsia. Acta Palaeontologica Polonica 48 (2): 261–272.

625   Zanno LE, Sampson SD. 2005. A new oviraptorosaur (Theropoda, Maniraptora) from the Late Cretaceous

626   (Campanian) of Utah. Journal of Vertebrate Paleontology 25:897-904.

627   Zheng R, Farke A, Kim G. 2011. A photographic atlas of the pes from a hadrosaurine hadrosaurid

628   dinosaur. PalArch's Journal of Vertebrate Palaeontology 8: 1-12

629

630

631

632

633

634

635

636

637

638

639

640

641

642

643
644 **FIGURES**

645 Figure 1: RBCM P900, the holotype of *Ferrisaurus sustutensis*, was collected along the BC Rail line near

646 the intersection of Birdflat Creek and the Sustut River in 1971, in the Sustut Basin of northern British

647 Columbia, Canada. Map modified from Evenchick et al. (2003).

648 Figure 2: Preserved elements of RBCM P900, holotype of *Ferrisaurus sustutensis,* in white (grey

649 represents missing parts of incomplete bones). RBCM P900 includes a partial right coracoid, partial left

650 scapular blade, complete left radius, partial left ulna, partial left tibia, fibula, and coossified astragalus

651 and ?calcaneum, partial left metatarsals I-IV, and digits III (phalanges 2-4) and IV (phalanges 2-5) of the

652 right pes.

653 Figure 3: Pectoral elements of RBCM P900, holotype of *Ferrisaurus sustutensis*, compared to other

654 Laramidian leptoceratopsids. A) Fragmentary right coracoid of RBCM P900 in lateral view, compared to

655 B) complete right scapulocoracoid of CMN 8889, *Leptoceratops gracilis*, lateral view centered on

656 coracoid with scapula in oblique view. Fragmentary left scapular blade of RBCM P900 in C) lateral and D)

657 medial view, compared to E) left scapula of MOR 300, *Cerasinops hodgskissi* in medial view, and F) left

658 scapula of TCM 2003.1.9, *Prenoceratops pieganensis* in lateral view. Abbreviations: sp - sternal process.

659 Figure 4. Radius of RBCM P900, holotype of *Ferrisaurus sustutensis*, compared to other Laramidian

660 leptoceratopsids. RBCM P900, *Ferrisaurus sustutensis*, left radius in A) lateral, B) medial, C) proximal,

661 and D) distal view. E) CMN 8889, *Leptoceratops gracilis*, left radius in lateral view. F) MOR 300,

662 *Cerasinops hodgskissi*, ?left radius in ?lateral view. Abbreviations: tb - tubercle.

663 Figure 5: Ulna of RBCM P900, holotype of *Ferrisaurus sustutensis*, compared to other Laramidian

664 leptoceratopsids. RBCM P900, *Ferrisaurus sustutensis*, left ulna in A) medial and B) distal view. C) CMN

665 8889, *Leptoceratops gracilis*, left ulna in medial view. D) MOR 300, *Cerasinops hodgskissi*, right ulna in

666 medial view. E) TCM 2003.1.8, *Prenoceratops pieganensis*, right ulna in medial view. F) MOR 452,

667 *Montanoceratops cerorhynchus*, right ulna in medial view. G) RBCM P900, *Ferrisaurus* left ulna in

668 posterior view; arrow indicates medial bend to distal ulna. H) TCM 2003.1.8, *Prenoceratops* right ulna in

669 anterior view. I) MOR 452, *Montanoceratops* right ulna in anterior view.

670 Figure 6: Tibia of RBCM P900, holotype of *Ferrisaurus sustutensis*, compared to other Laramidian

671 leptoceratopsids. RBCM P900, *Ferrisaurus* left tibia in A) medial, B) and C) posterior, D) anterior, and E)

672 lateral views, and F and G) block removed from anterior face of tibia containing four partial metatarsals.

673   The dashed line in C) delineates the possible boundary of the astragalus/calcaneum on the tibia, and the

674   dashed lines in E) indicate the preserved metatarsals in cross-section. CMN 8889, *Leptoceratops gracilis*

675   left tibia in H) posterior and I) anterior view. MOR 300, *Cerasinops hodgskissi* right tibia in J) anterior and

676   K) posterior views, and L) left tibia in posterior view. Abbreviations: as - astraglus, ca - calcaneum, fib -

677   fibula, ma - matrix, mt - metatarsal.

678   Figure 7: Pedal elements of RBCM P900, holotype of *Ferrisaurus sustutensis*, compared to other

679   Laramidian small-bodied ornithischians. RBCM P900, *Ferrisaurus*, left digit III in A) medial and B) lateral

680   views, and C) left digit IV in lateral view. D) MOR 542, *Montanoceratops cerorhynchus*, right digit IV in

681   lateral view. Illustrations of E) RBCM P900, *Ferrisaurus*, F) CMN 8889, *Leptoceratops gracilis*, G) MOR

682   300, *Cerasinops hodgskissi*, H) MOR 542, *Montanoceratops cerorhynchus*, in dorsal view, and I) ROM

683   804, *Parksosaurus warreni*.

684   Figure 8: Results of the phylogenetic analyses showing the relationships of *Ferrisaurus sustutensis* within

685   Ceratopsia. A) Strict consensus tree using the matrix modified from He et al. (2015). B) Strict consensus

686   tree using the matrix from Morschhauser et al. (2019).

Figure 1

RBCM P900, the holotype of Ferrisaurus sustutensis, was collected along the BC Rail line near the intersection of Birdflat Creek and the Sustut River in 1971, in the Sustut Basin of northern British Columbia, Canada.

Map modified from Evenchick et al. (2003).
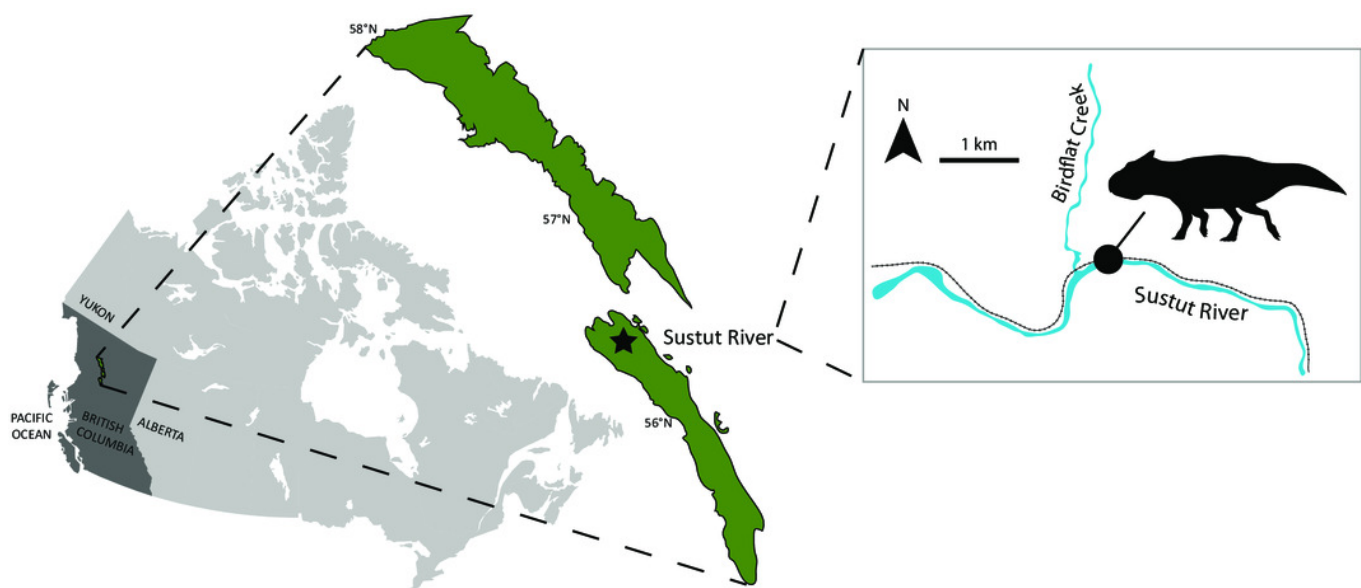
Figure 2

Preserved elements of RBCM P900, holotype of Ferrisaurus sustutensis, in white (grey represents missing parts of incomplete bones).

RBCM P900 includes a partial right coracoid, partial left scapular blade, complete left radius, partial left ulna, partial left tibia, fibula, and coossified astragalus and ?calcaneum, partial left metatarsals I-IV, and digits III (phalanges 2-4) and IV (phalanges 2-5) of the right pes.
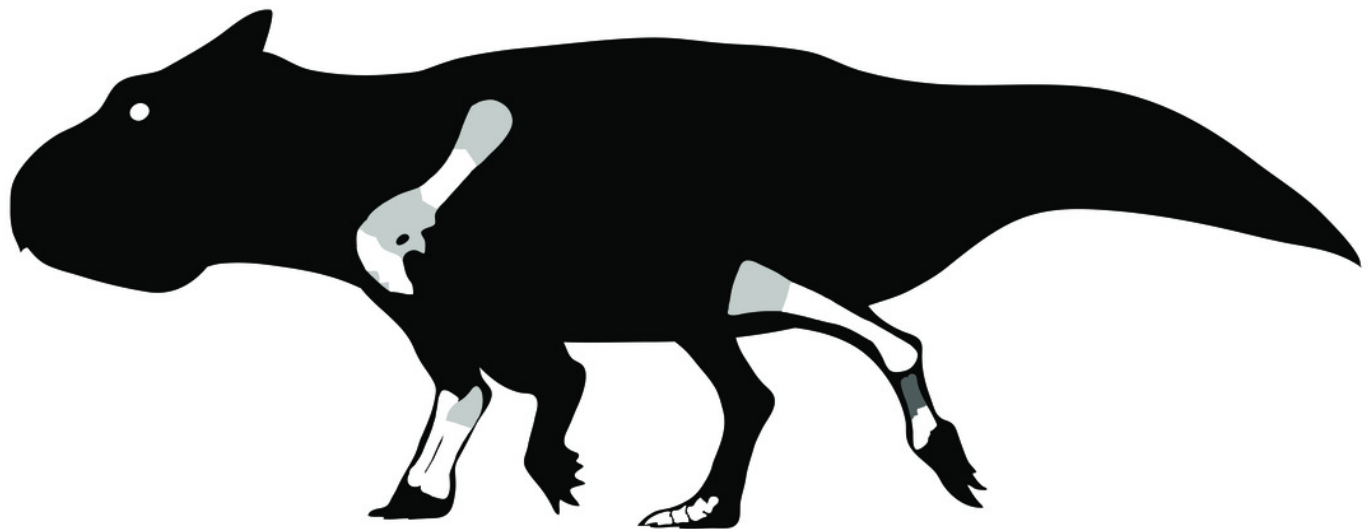
Figure 3

Pectoral elements of RBCM P900, holotype of *Ferrisaurus sustutensis*, compared to other Laramidian leptoceratopsids.

A) Fragmentary right coracoid of RBCM P900 in lateral view, compared to B) complete right scapulocoracoid of CMN 8889, *Leptoceratops gracilis*, lateral view centered on coracoid with scapula in oblique view. Fragmentary left scapular blade of RBCM P900 in C) lateral and D) medial view, compared to E) left scapula of MOR 300, *Cerasinops hodgskissi* in medial view, and F) left scapula of TCM 2003.1.9, *Prenoceratops pieganensis* in lateral view.

Abbreviations: sp - sternal process.
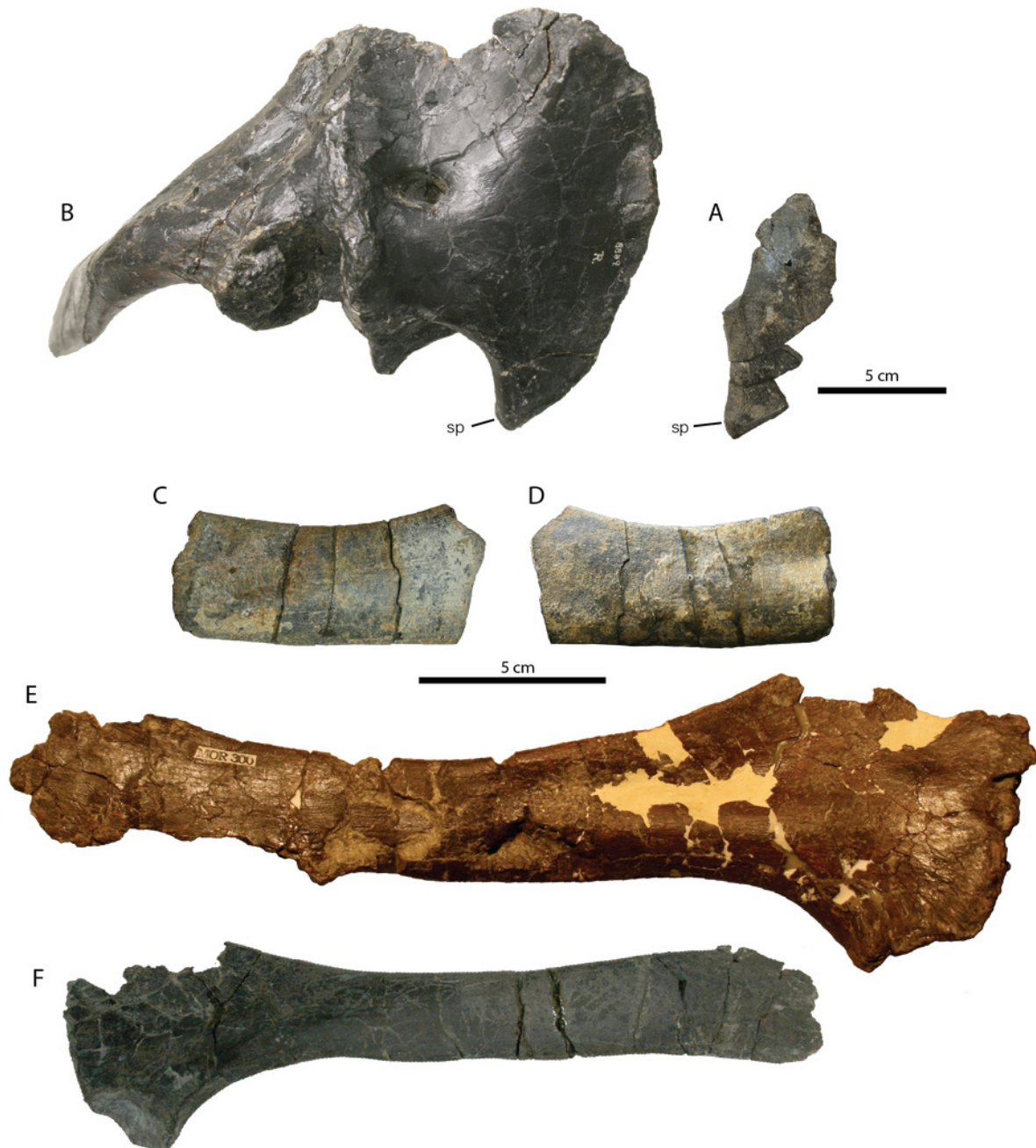
Figure 4

Radius of RBCM P900, holotype of Ferrisaurus sustutensis, compared to other Laramidian leptoceratopsids.

RBCM P900, Ferrisaurus sustutensis, left radius in A) lateral, B) medial, C) proximal, and D) distal view. E) CMN 8889, Leptoceratops gracilis, left radius in lateral view. F) MOR 300, Cerasinops hodgskissi, ?left radius in ?lateral view. Abbreviations: tb - tubercle.

Figure 5

Ulna of RBCM P900, holotype of Ferrisaurus sustutensis, compared to other Laramidian leptoceratopsids.

RBCM P900, Ferrisaurus sustutensis, left ulna in A) medial and B) distal view. C) CMN 8889, Leptoceratops gracilis, left ulna in medial view. D) MOR 300, Cerasinops hodgskissi, right ulna in medial view. E) TCM 2003.1.8, Prenoceratops pieganensis, right ulna in medial view. F) MOR 452, Montanoceratops cerorhynchus, right ulna in medial view. G) RBCM P900, Ferrisaurus left ulna in posterior view; arrow indicates medial bend to distal ulna. H) TCM 2003.1.8, Prenoceratops right ulna in anterior view. I) MOR 452, Montanoceratops right ulna in anterior view.

5 cm

Figure 6

Tibia of RBCM P900, holotype of Ferrisaurus sustutensis, compared to other Laramidian leptoceratopsids.

RBCM P900, Ferrisaurus left tibia in A) medial, B) and C) posterior, D) anterior, and E) lateral views, and F and G) block removed from anterior face of tibia containing four partial metatarsals. The dashed line in C) delineates the possible boundary of the astragalus/calcaneum on the tibia, and the dashed lines in E) indicate the preserved metatarsals in cross-section. CMN 8889, Leptoceratops gracilis left tibia in H) posterior and I) anterior view. MOR 300, Cerasinops hodgskissi right tibia in J) anterior and K) posterior views, and L) left tibia in posterior view. Abbreviations: as - astraglus, ca - calcaneum, fib - fibula, ma - matrix, mt - metatarsal.

Figure 7

Pedal elements of RBCM P900, holotype of Ferrisaurus sustutensis, compared to other Laramidian small-bodied ornithischians.

RBCM P900, Ferrisaurus, left digit III in A) medial and B) lateral views, and C) left digit IV in lateral view. D) MOR 542, Montanoceratops cerorhynchus, right digit IV in lateral view. Illustrations of E) RBCM P900, Ferrisaurus, F) CMN 8889, Leptoceratops gracilis, G) MOR 300, Cerasinops hodgskissi, H) MOR 542, Montanoceratops cerorhynchus, in dorsal view, and I) ROM 804, Parksosaurus warreni.
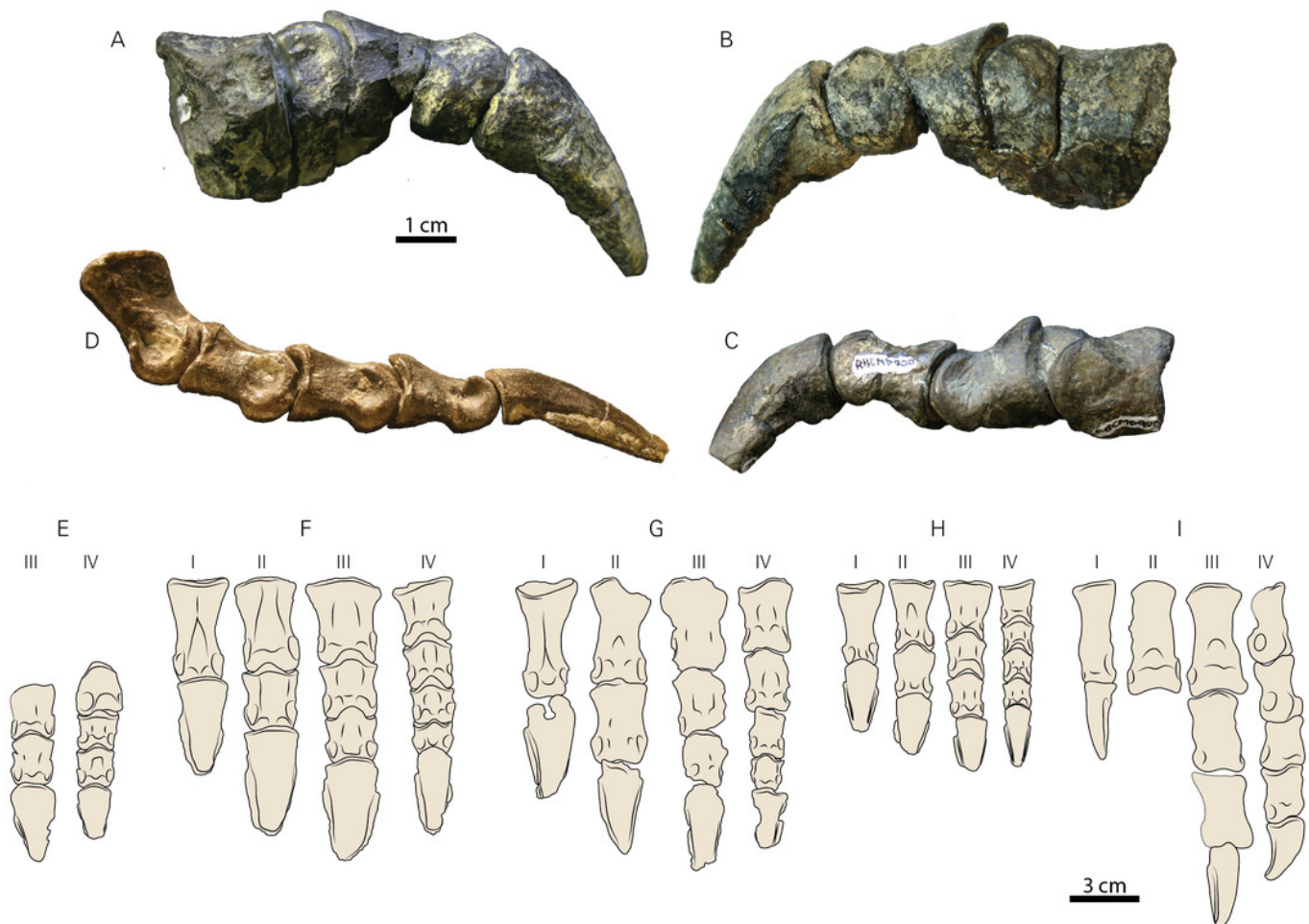
Figure 8

Results of the phylogenetic analyses.

Strict consensus trees showing the relationships of Ferrisaurus sustutensis within Ceratopsia: A) Strict consensus tree using the matrix modified from He et al. (2015). B) Strict consensus tree using the matrix from Morschhauser et al. (2019).
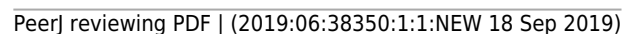
Table 1: Selected measurements of forelimb and hindlimb elements in leptoceratopsids (mm).

1   Table 1: Selected measurements of forelimb and hindlimb elements in leptoceratopsids (mm).

Taxon	Specimen	Radius	Ulna		Tibia		Fibula	Measurement source
		Length	Length	Distal width	Length	Distal width	Length	
Ferrisaurus sustutensis	RBCM P900	135.0		38.2		90.1		Direct measurement
Cerasinops hodgskissi	MOR 300 R		201.4	>32.6	363.0	~86.3	337.0	Direct measurement
	MOR 300 L					95.0		Direct measurement
	USNM 13863				200	62		Brown and Schlaikjer (1942)
Ischioceratops zhuchengensis	ZCFM V0016				329			He et al. (2015)
Leptoceratops gracilis	AMNH 5205	167	224			117		Sternberg (1951)
	CMN 8887	115			240			Sternberg (1951)
	CMN 8888	137			290			Sternberg (1951)
	CMN 8889 L	160.5	202.5	35.7	323.0	87.9	293.0	Direct measurement
	PU 18133				~385	~78		Ostrom (1978)
Montanoceratops cerorhynchus	AMNH 5464				355	102		Brown and Schlaikjer (1942)
	MOR 542			28.6	249.2	50.6	235.9	Direct measurement
Prenoceratops pieganensis	TCM 2003.1.8		143.3	19.1				Direct measurement

3
4

Table 2. Lengths of phalanges from pedal digits III and IV in leptoceratopsids (mm).

1   Table 2. Lengths of phalanges from pedal digits III and IV in leptoceratopsids (mm).

Taxon	Specimen	III			IV				Measurement source
		2	3	4	2	3	4	5	
Ferrisaurus sustutensis	RBCM P900	28.1	28.3	40.7	24.4	21.1	22.3	29.3	Direct measurement
Cerasinops hodgskissi	MOR 300 R	?34.1	?27.9			?25.4			Direct measurement
	MOR 300 L	36.5	29.8	44.9	33.5	27.2	20.1	>31.1	Direct measurement
	USNM 13863	27.5	29.5	41	21	21	18.5		Brown and Schlaikjer (1942)
Leptoceratops gracilis	CMN 8887	21.3	16.5	32.2	18.4	14.4	13.7	24.9	Direct measurement from cast
	CMN 8889 R	31.9	29.6	51.0	29.4	25.1	22.0	44.1	Direct measurement
	PU 18133	40	30		32	~26	~20		Ostrom (1978)
Montanoceratops cerorhynchus	AMNH 5464	33		68					Brown and Schlaikjer (1942)
	MOR 542	28.4	25.1	~29.0	20.4	21.0	19.1	34.0	Direct measurement